



PERGAMON

Scripta Materialia 45 (2001) 1321–1326



www.elsevier.com/locate/scriptamat

Yielding and flow behavior of Mo_5Si_3 single crystals

K. Yoshimi^{a,*1}, M.H. Yoo^a, A.A. Wereszczak^a, S.M. Borowicz^b,
E.P. George^a, and R.H. Zee^b

^a*Metals and Ceramics Division, Oak Ridge National Laboratory, Oak Ridge, TN 37831-6115, USA*

^b*Materials Engineering Program, Auburn University, Auburn, AL 36849, USA*

Received 14 May 2001

Abstract

Deformation behavior of Mo_5Si_3 was studied using single crystals under compression. It was found that yielding and flow behavior were strongly dependent on temperature, strain rate and crystal orientation. A stress exponent and an activation enthalpy of lower yield stresses were estimated to be ≈ 6 and 4.5 eV, respectively. © 2001 Acta Materialia Inc. Published by Elsevier Science Ltd. All rights reserved.

Keywords: Intermetallics; Molybdenum silicide; Slip; Yield phenomena

Introduction

Molybdenum silicides are very attractive for high temperature applications not only as structural components, but also as heating elements and oxidation-resistant surface coating materials. Considerable research on MoSi_2 has been motivated because of its good high temperature strength, electrical resistivity and oxidation resistance [1]. Since it was found that the addition of a small amount of boron dramatically improved oxidation resistance of D8_m -type Mo_5Si_3 [2,3], which has a tetragonal structure with $I4/mcm$ symmetry (see Fig. 1), attention has shifted to the silicides containing higher Mo concentrations [4–10].

Mechanical property of monolithic Mo_5Si_3 was first reported by Mason and Van Aken in 1995 [9]. In their work [9], an activation energy of 510 kJ mol^{-1} and stress exponent of 6 for creep deformation were determined using single crystals. They also observed $\langle 110 \rangle$ -type dislocations, which likely contributed to creep deformation in the Mo_5Si_3 lamellae of MoSi_2 – Mo_5Si_3 eutectic. Recently, Chu et al. studied physical and

* Corresponding author.

E-mail address: yoshimi@imr.tohoku.ac.jp (K. Yoshimi).

¹ Present address: Institute for Materials Research, Tohoku University, Sendai, Miyagi 980-8577, Japan.

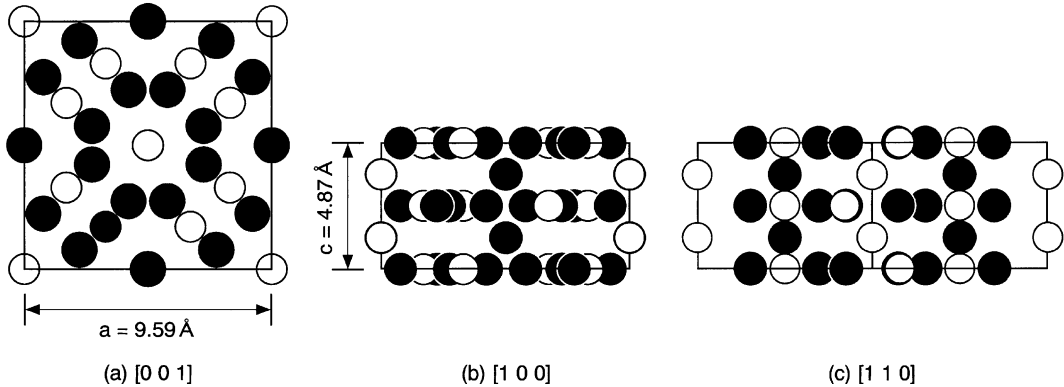


Fig. 1. Atomic structure of Mo_5Si_3 compound in views along (a) [0 0 1], (b) [1 0 0] and (c) [1 1 0] directions. Closed circles correspond to molybdenum atoms and open ones silicon atoms. Lattice parameters were quoted from the Ref. [10].

mechanical properties theoretically and experimentally using single crystals [10]. Important findings in their work [10] are that the thermal expansion is strongly anisotropic along the a and c directions and the elastic moduli are less anisotropic than that of most transition metal disilicides. However, yielding and deformation behavior of Mo_5Si_3 are still unknown. Therefore, the purpose of this work is to first investigate them using single crystals.

Experimental details

Mo_5Si_3 was produced by arc melting in an argon atmosphere, and drop-cast into a cylindrical copper mold of ≈ 6 mm in diameter and 120 mm in length. A single crystal was grown from the drop-cast ingot in an optical floating zone furnace at a growth rate of 10 mm/h and a rotation speed of 20 rpm in flowing argon gas (flow rate; 4 L min^{-1}). The growth direction of the single crystal was near [1 0 1]. In the single crystal, Mo:Si atomic ratio is approx. 61.8:38.2, and oxygen and carbon contents are approx. 0.01 and 0.001 mass%, respectively. Other impurities are as small as in wt.ppm order. Compression specimens with three different axes, [0 0 1], near [1 0 1] (the growth direction) and [1 0 0], were cut from the single crystal by an electro-discharge machine (EDM). The dimension of the specimen was $\approx 1.7 \times 1.7 \times 4 \text{ mm}^3$. Surfaces of the specimens were mechanically and then vibratorily polished to remove heat-damaged layer introduced by EDM, and finally wiped with Murakami etch to eliminate contamination on the polished surfaces. Compression tests were performed at temperatures between 1473 and 1723 K, corresponding to 0.6 to 0.7 of the melting point of stoichiometric Mo_5Si_3 [11], in an argon gas atmosphere with a flow rate of about 50 ml min^{-1} . Slip traces on the surfaces were observed by optical microscopy (OM) using Nomarski interference contrast, and operative slip planes were investigated by the two-surfaces trace analysis method.

Results and discussion

Fig. 2 shows stress–strain curves obtained at an initial strain rate of $1.7 \times 10^{-4} \text{ s}^{-1}$ for the three axes. For the near $[101]$ orientation, a large yield drop occurs after yielding at and above 1523 K, and a lower yield point appears (Fig. 2(a)). At 1473 K, specimens failed by brittle fracture under an elastic regime. Thus, there is the brittle–ductile transition (BDT) between 1473 and 1523 K at the strain rate for this orientation. At temperature between 1573 and 1673 K, strain-rate cycling tests were performed after the lower yield points. The strains where the cross-head speed was decreased by a factor of ten are denoted by downward arrows in Fig. 2(a). After a few percent of additional plastic strain, the cross-head speed was increased by a factor of hundred. The strains are also denoted by upward arrows. From these strain-rate cycling tests, it is found that the lower yield and flow stresses have strong strain-rate sensitivity. For the $[100]$ orientation, similar yielding and deformation behavior to those for the near $[101]$ orientation, i.e. a large yield drop followed by a lower yield point, were observed at 1673 and 1723 K, as shown in Fig. 2(b). At 1573 K, the specimen failed without a lower yield point after yielding. Thus, BDT is likely to be around 1573 K at the strain rate for this

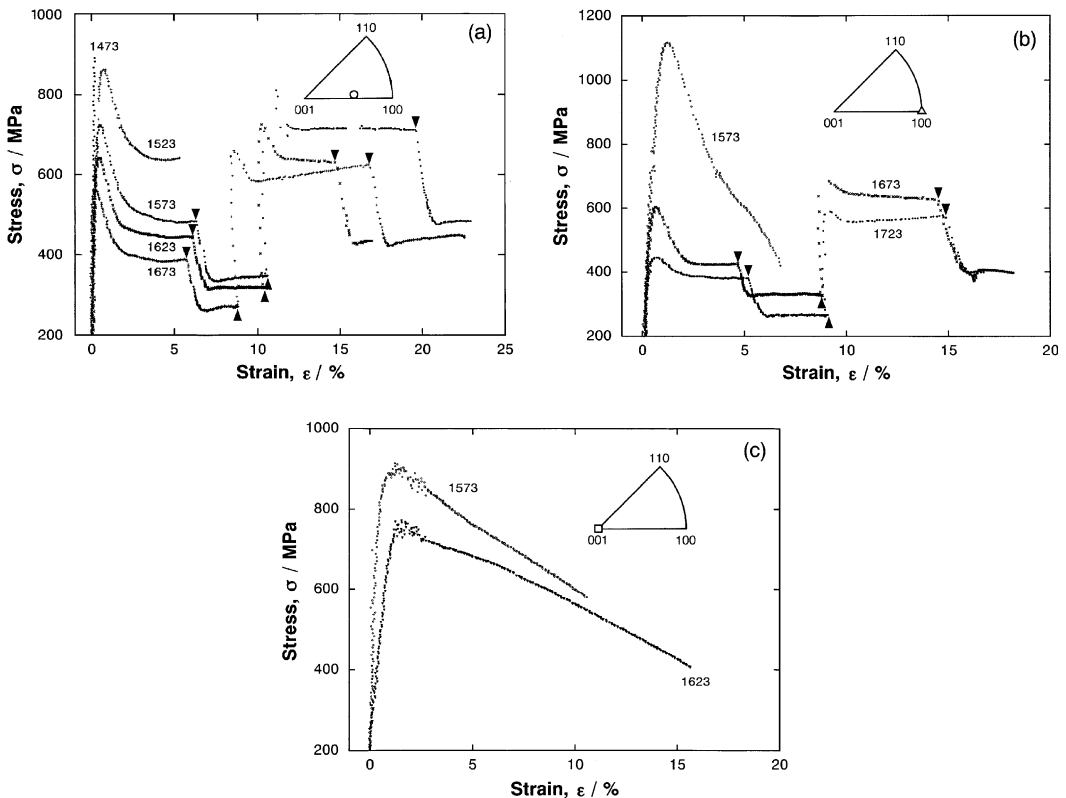


Fig. 2. Stress–strain curves of Mo_5Si_3 single crystals for (a) near- $[101]$ orientation (growth direction), (b) $[100]$ and (c) $[001]$ orientations.

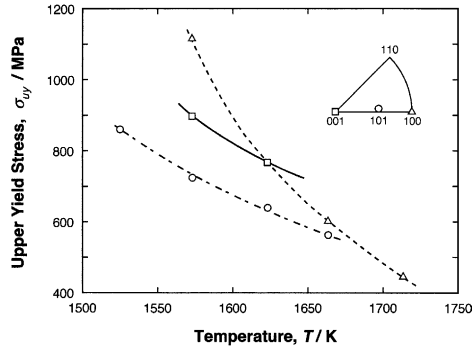


Fig. 3. Temperature dependence of upper yield stress for the three orientations.

orientation. The strain-rate cycling tests were also carried out at 1673 and 1723 K for the [100] orientation, and the lower yield and flow stresses were also strongly dependent on strain rate in the similar manner for the near [101] orientation. On the other hand, upper and lower yield points did not appear for the [001] orientation at temperatures examined (Fig. 2(c)). After yielding, the flow stress gradually decreased, but no failure occurred even at relatively large amounts of strain. The specimens for this orientation, in all these tests, largely leaned from the original vertical direction. This should be the cause why the flow stress decreased monotonously after yielding.

The upper yield stresses for the three orientations are shown as a function of temperature in Fig. 3. The stresses exhibit strong orientation dependence, and that for the near [101] was the lowest among the three orientations in the examined temperature range.

Fig. 4 shows optical micrographs of slip traces on the surfaces of the specimens deformed at 1623 K and a few percent plastic strains. For the near [101] and [100]

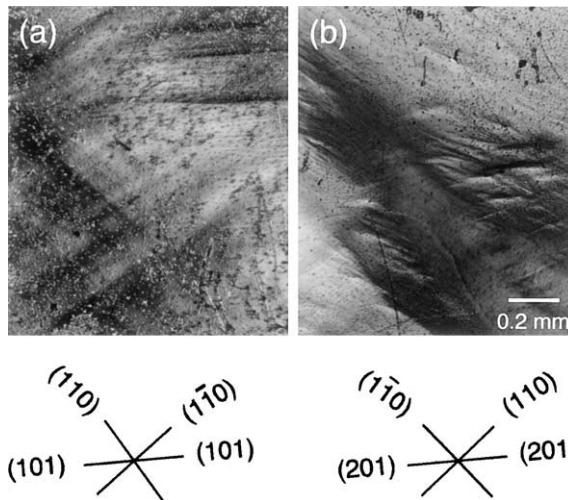


Fig. 4. Slip traces on specimen surfaces observed by OM: (a) near-[101] and (b) [100] orientations.

Table 1
Schmid factors for the four possible slip systems in the [1 0 1] orientation

	(001)[1 1 0]	(100)[00 1]	(1 1 0)[00 1]	(1 $\bar{1}$ 0)[00 1]
[1 0 1]	0.331	0.442	0.331	0.288

orientations, apparent slip traces were seen on the surfaces, whereas, for the [00 1] orientation, no observable trace appeared at any temperature. The traces are relatively homogeneous and straight for the near [1 0 1] orientation. On the other hand, the traces for the [1 0 0] orientation are inhomogeneous and locally wavy, suggesting the occurrence of cross-slipping. By the two-surfaces trace analysis, {1 1 0} plane slips were identified for both the orientations. In addition, traces of relatively low index planes, e.g. (1 0 1) and (2 0 1), were observed for the near [1 0 1] and [1 0 0] orientations, respectively.

The orientation dependence of the upper yield stresses should be associated with the resolved shear stresses for operative slip systems. Possible slip systems in the Mo_5Si_3 compound have been proposed by Mason and Van Aken [9] and Chu et al. [10]: they are (001)(1 1 0), {100}[00 1] and {110}[00 1]. The Schmid factors for the slip systems are tabulated for the [1 0 1] orientation in Table 1. The Schmid factors for the four possible slip systems are zero along the [1 0 0] and [00 1] axes. These should give higher upper yield stresses for the [1 0 0] and [00 1] orientations than for the near [1 0 1] orientation, as seen in Fig. 3. As mentioned above, however, the yielding behavior and appearance of slip traces were totally different between the [1 0 0] and [00 1] orientations. Other unknown slip systems may be operative for the [1 0 0] and/or [00 1] orientations. In addition, it is very difficult at present to give definite interpretation about the slips activated on the (1 0 1) and (2 0 1) planes. Further studies of slip behavior are needed.

The relation between the lower yield stresses and the strain rates was examined for the near [1 0 1] and [1 0 0] orientations through the strain-rate cycling tests. Strain-rate sensitivity parameters of the lower yield stresses are almost the same for the two orientations regardless of temperature in the present test condition, and the average of the parameters is approx. 0.164. This value gives a stress exponent of about 6 by $n = 1/m$, which is in excellent agreement with that obtained Mason and Van Aken [9]. Considering that the lower yield stresses, τ_{ly} , are related to the thermal activation process with the stress exponent by $\tau_{ly} = A\dot{\epsilon}^{1/n} \exp(Q/RT)$, the activation enthalpy of about 4.5 eV is estimated for the lower yield stresses at the strain rate of $1.7 \times 10^{-4} \text{ s}^{-1}$.

The mechanical properties of the Mo_5Si_3 single crystals observed in this study are similar to those of semiconductors such as Si, Ge, and III–V compounds [12–14], suggesting they are governed by the basically same mechanisms. In general, the stress exponents of lower yield stress are high in those semiconductors (1–4), since the slip mechanism is controlled by high Peierls stress. The obtained stress exponent of Mo_5Si_3 is also high, similar to those of the semiconductors. Furthermore, the obtained activation enthalpy of the lower yield stresses is one order of magnitude higher than those of the semiconductors. The high stress exponent and higher activation enthalpy should

be due to high Peierls stress attributable to the complex, anisotropic atomic structure of the Mo_5Si_3 compound (Fig. 1).

Conclusions

In this study, yielding and deformation behavior of D8_m -type Mo_5Si_3 were first investigated using single crystals in compression, and it is found that they were strongly dependent on the crystal orientations. The upper and lower yield phenomenon appeared at and above 1523 K for the near $[101]$ orientation and above 1573 K for the $[100]$ one. At lower temperature, the single crystals failed at the strain-rates of 10^{-4} s^{-1} , indicating the BDT. The plastic deformation proceeded by slip under the test conditions. The $\{110\}$ -plane traces were observed on the surfaces as one of operative slip planes. In addition, relatively low index planes, e.g. (101) and (201) , were also observed. The thermal activation process of the lower yield stresses was analyzed. The stress exponent of the lower yield stresses of 6 was estimated for the near $[101]$ and $[100]$ orientations, and the activation enthalpy of 4.5 eV for the near $[101]$ orientation.

Acknowledgements

The authors would like to thank Prof. I. Yonenaga of Institute for Materials Research, Tohoku University for his useful discussion. This research was sponsored by the Division of Materials Science and Engineering, Office of Basic Energy Sciences, US Department of Energy, under contract of DE-AC05-00OR22725 with UT-Battelle, LLC.

References

- [1] Vasudévan, A. K., & Petrovic, J. J. (1992). *Mater Sci Eng A* 155, 1.
- [2] Meyer, M. K., & Akinc, M. (1996). *J Am Ceram Soc* 79, 938.
- [3] Meyer, M. K., & Akinc, M. (1996). *J Am Ceram Soc* 79, 2763.
- [4] Meyer, M. K., Kramer, M. J., & Akinca, M. (1996). *Intermetallics* 4, 273.
- [5] Schneibel, J. H., Liu, C. T., Easton, D. S., & Carmichael, C. A. (1999). *Mater Sci Eng A* 261, 78.
- [6] Schneibel, J. H., Liu, C. T., Heatherly, L., & Kramer, M. J. (1998). *Scripta Mater* 38, 1169.
- [7] Misra, A., Petrovic, J. J., & Mitchell, T. E. (1999). *Scripta Mater* 40, 191.
- [8] Nunes, C. A., Sakidja, R., & Perepezko, J. H. (1997). In M. V. Nathal, R. Darolia, C. T. Liu, P. L. Martin, D. B. Miracle, R. Wagner, & M. Yamaguchi (Eds.). *Structural Intermetallics* (p. 831). Warrendale, PA: TMS.
- [9] Mason, D. P., & Van Aken, D. C. (1995). *Acta Metall Mater* 43, 1201.
- [10] Chu, F., Thoma, D. J., McClellan, K., Peralta, P., & He, Y. (1999). *Intermetallics* 7, 611.
- [11] Massalski, T. B., Murray, J. L., Bennett, L. H., & Baker, H. (Eds.). (1986). *Binary Alloy Phase Diagrams* (Vol. 2, p. 1632). Metals Park, Ohio: ASM.
- [12] Kojima, K., & Sumino, K. (1971). *Cryst Latt Def* 2, 147.
- [13] Yonenaga, I., & Sumino, K. (1978). *Phys Stat Sol (A)* 50, 685.
- [14] Yonenaga, I. (1997). *J Phys III* 7, 1435.